NIH-PA Author Manuscript

Endothelial IL-1R1 is a critical mediator of EAE pathogenesis

Qiming Li[*], **Nicole Powell**[*], **Hao Zhang**, **Natalya Belevych**, **San Ching**, **Qun Chen**, **John Sheridan**, **Caroline Whitacre**, and **Ning Quan**[*]

Institute of Behavior Medicine, 3132 Postle Hall, 305 West 12th Avenue, Ohio State University, Columbus, OH 43210-1094, USA

Abstract

Interleukin-1 (IL-1) has been implicated in the disease progression of multiple sclerosis (MS). In the animal model of MS, experimental autoimmune encephalomyelitis (EAE), the induction of disease is significantly attenuated in mice lacking the type I IL-1 receptor (IL-1R1). In this study, we created a transgenic mouse (eIL-1R1 kd) in which IL-1R1 expression is knocked down specifically in endothelial cells. Induction of EAE in eIL-1R1 kd mice results in a decrease in incidence, severity and delayed onset of EAE. In addition, eIL-1R1 kd mice show significant decrease in VCAM-1 expression and diminished CD45^{+} and CD3^{+} infiltrating leukocytes in the spinal cord in animals challenged with EAE. Further, IL-1 and IL-23 stimulate IL-17 production by splenocytes from both wild type and the eIL-1R1 kd animals. Similarly, IL-1 and IL-23 synergistically stimulate splenocytes proliferation in these two strains of animals. After immunization with MOG_{79-96}, although eIL-1R1 kd mice displayed greatly reduced clinical scores, their splenocytes produced IL-17 and proliferated in response to a second MOG challenge, similar to wild type animals. These findings indicate a critical role for endothelial IL-1R1 in mediating the pathogenesis of EAE, and describe a new model that can be used to study endothelial IL-1R1.

Introduction

Interleukin-1 (IL-1) is an important cytokine in inflammation and immunoregulation (Dinarello, 2009). Its relevance in multiple sclerosis (MS) has been amply demonstrated. Gene polymorphisms (Dincic *et al.*, 2006) and/or dysrgeulated levels of IL-1, changes in the receptor for IL-1 (IL-1R) and changes in the naturally produced IL-1 receptor antagonist (IL-1Ra) have all been implicated in the pathology of MS. For example, elevated levels of IL-1β levels have been found in the white matter and in acute lesions (Brosnan *et al.*, 1995), cerebrospinal fluid, and sera (Hauser *et al.*, 1990; Tsukada *et al.*, 1991) of MS patients. In addition, microglial cells as well as hematogenous macrophages entering the central nervous system (CNS) in patients with MS secrete high levels of IL-1β (Cannella and Raine, 1995). An increased risk of MS has also been observed in families that have higher production ratios of IL-1β over its naturally occurring IL-1Ra (Ahmed *et al.*, 2002). In general, increased IL-1 activity is associated with more severe MS symptoms.

[*]Corresponding author. Tel: 614-292-1657; fax: 614-247-6945. Quan.14@osu.edu (N. Quan)..

In the animal model of MS, experimental autoimmune encephalomyelitis (EAE), the induction and progression of the disease are significantly attenuated in mice deficient of the type I IL-1 receptor (IL-1R1) (Schiffenbauer *et al.*, 2000) (Sutton *et al.*, 2006), suggesting IL-1R1 might be a therapeutic target of EAE. Whether this target can be further restricted to IL-1R1 expressed on a specific cell type has not been reported.

The vast majority of IL-1R1 in the brain is found on the endothelial surface, with some IL-1R1 on neurons in the select few brain regions (Ericsson *et al.*, 1995). Endothelial IL-1R1 has been shown to mediate many IL-1-mediated effects in the CNS (Ching *et al.*, 2007). The binding of IL-1 to the endothelial IL-1R1 is known to activate endothelial cells and mediates recruitment of leukocytes into the brain through the upregulation of cell adhesion molecules (CAMs) and cytokines (Hubbard and Rothlein, 2000) (Ching *et al.*, 2005). Therefore, endothelial IL-1R1-mediated leukocyte recruitment may be critical in the induction and progression of MS. In this study, we tested the effect of selective knockdown of the expression of endothelial IL-1R1 on the disease course of EAE.

Materials and Methods

Transgenic constructs

The transgenic construct is built from a construct containing Tie-2 promoter (2 kb)-rtTA-Tie2 enhancer (10 kb) (Tie2-rtTA) that we built in a previously study (Ching *et al.*, 2007). In the current study, the rtTA sequence of the Tie2-rtTA is replaced by the sequence of an antisense cDNA of IL-1R1. To this end, cDNA was generated from reverse transcription of total RNA from mouse brain. Then, PCR amplification was performed with the following primers: 5'-TGGCGCGCCAACGTGAGCTTCTTCGGAGT -3' and 5'-GTTAATTAAAGGAGTCCCTGTACCAAAGCAC -3'. These primers flank the exon5-exon9 region of the murine IL-1R1 mRNA. Restriction sites, PacI or AscI, were added to the 5' end of these primers to facilitate later ligation reaction. The resulting product is a partial cDNA sequence of mIL-1R1 (GenBank accession no. NM_008362; nucleotides 1343–744), with the PacI and AscI sites flanking the sequence. The Tie2-rtTA was digested with PacI and AscI to excise the rtTA sequence; the gap so created was filled by ligating the IL-1R1 cDNA fragment (in the antisense direction) between the Tie2 promoter and enhancer. This construct is designated as the Tie2-antiIL-1R1. A linker sequence (L) exists immediately after the antiIL-1R1 sequence in the construct; this sequence is retained from the original Tie2-rtTA construct. The Tie2-antiIL-1R1 construct was linearized by restriction digest with SalI before it was injected into fertilized eggs. The transgenic construct is shown in Figure 1A.

Tie2-GFP construct was kindly provided by Dr. Tom Sato (Department of Internal Medicine and Molecular Biology, University of Texas Southwestern Medical Center, Dallas, TX). Transgenic animals made from this construct showed universal expression of GFP in endothelial cells throughout the body (Motoike *et al.*, 2000).

Generation of transgenic lines

All experiments were conducted in accordance with the NIH guide on the care and use of animals for research, and an in-house protocol approved by the Ohio State University Animal Care and Use Committee. All experiments were designed to minimize the number of animals used and to maximize the comfort of the animals.

The Tie2-antiIL-1R1 and Tie2-GFP constructs were co-injected into fertilized eggs (FVB zygotes) at 3:1, 1:1, and 1:3 molar ratios. Real-time PCR primer-probe sets, 5'-GGTCGCTACCATTACCAGTTGG/5'-CCTCTACAGATGTGATATGGCTGATT, and probe 5'-CTGGTGTCAAAAATAATAATAACCGGGCAGGG; and 5'-

TGGTCCCAATTCTCGTGGAA/5'-CTCTCCGCTGACAGAAAATTTGT and probe 5'-TGGATGGCGATGTGAATGGG were used to detect the presence of the Tie2-antiIL-1R1 (the target sequence is the linker sequence that is unique to the Tie2-antiIL-1R1 transgene) or the GFP transgene, respectively. Two functional lines were identified out of 49 founder animals. One of the lines was stable for several generations and demonstrated consistent desired phenotypic responses. This line was used in this study and referred to as the eIL-1R1 knockdown (eIL-1R1 kd) mouse.

Phenotype characterization of eIL-1R1 kd animal

The cell type specific expression of the transgenes was determined by examination of the appearance of GFP in the transgenic animals. Mice were anesthetized with 2 mg/20 g Nembutal (Abbott Laboratories, North Chicago, IL) and perfused with 20 ml cold PBS followed by 25 ml cold 4% PFA/PBS. Brain, liver, lung, thymus and spleen were dissected and post fixed in 4% PFA for 2 h and then stored in 25% sucrose at 4°C. Tissues were cut by a microtome to 40-μm thick sections and examined by a fluorescent microscope (BX51; Olympus, Melville, NY). The consistency of the phenotype was examined over 5 generations in the transgenic mice.

To verify transgene expression in endothelial cells, tissue sections were first photographed for GPF. Then they were heated in an antigen retrieval buffer (10 mM Sodium Citrate, 0.05% Tween 20, pH 6.0) at 95°C for 30 min. They were then washed in PBS-tween 20 buffer 3 times, before they were incubated with a rat anti-PECAM antibody (DIA310, Dianova, Hamburg, Germany) at 1:20 for 2 h at room temperature. The sections were then incubated with a C3-labeled rabbit anti-rat antibody (Jackson ImmunoResearch Laboratories). Co-localization of GFP and anti-PECAM was examined by fluorescence microscopy.

The mRNA expression of the transgenes was examined by reverse transcription-PCR analysis. Total RNA was extracted from the tail clip samples by conventional method. The RNA samples were digested with DNase I and reverse transcribed to generate cDNA samples. The same primer sets that were used for genotyping (described above) were used for the PCR amplification of the cDNA.

A hallmark effect of IL-1 when it acts on brain endothelial cells is the induction of cyclooxygenase-2 (COX-2) in these cells after IL-1 is injected into the cerebral ventricles (Proescholdt *et al.*, 2002). We used this effect to examine whether the functional consequences of IL-1 stimulation on brain endothelial cells are blocked in the eIL-1R1kd animals. Mice, eIL-1R1 kd transgenic mice and their FVB non-transgenic wild type (WT) littermates, weighing 20–30 g at the age of 6–10 weeks, were anesthetized by Nembutal (Abbott Laboratories, North Chicago, IL) and then securely fixed onto the small animal stereotaxic (David Kopf Instrument, Tujunga, CA). A 28 gauge guide cannula was then inserted into the lateral ventricle (lateral from midline, 1 mm; posterior to bregma, 0.7 mm; ventral from the skull, 2.7 mm) and secured on the skull with a glass polyalkenoate cement and sealed with a dummy injector (Plastic One, Roanoke, VA). After the animals recovered from the surgery for 2 days, murine IL-1β (20 ng in 10 μl; PeproTech, Rocky Hill, NJ) or saline was injected into the lateral ventricle. The animals were sacrificed 4 h later for immunohistochemical labeling of COX-2.

To determine whether IL-1R1 in non-endothelial cells was altered in the transgenic animals, in-cell Western Blot analysis of IL-1R1 in blood leukocytes were conducted. Transgenic (eIL-1R1 kd) and WT FVB littermates (n = 5 mice per group) were anesthetized with isoflurane (Abbott, North Chicago, IL, USA). Approximately 0.5 ml of whole blood was collected by cardiac puncture from each animal and diluted in 1 ml heparinized saline. The

blood samples were slowly layered onto Histopaque-1077 (Sigma) in a 15 ml centrifuge tube. After centrifugation at 400 *g* for 30 min at room temperature, the resulting interface layer containing leukocytes was carefully collected. The isolated leukocytes were washed twice with 10 ml of wash buffer (1% BSA/PBS with 0.05% NaN3) and centrifuged at 250 *g* for 10 min at room temperature. Cell pellets were then suspended in 1 ml of wash buffer and cell number was adjusted to 2×10^6 per milliliter. The leukocytes were then fixed in 1% paraformaldehyde on ice for 30 min. A total of 100 μl of the fixed leukocyte suspension was incubated with a rabbit anti-mouse IL-1R1 (Santa Cruz Biotechnology, Santa Cruz, CA) in 1:200 dilution on ice for 30 min. The samples were then washed and incubated with an infrared dye (IRdye 800CW)-labeled goat anti-rabbit antibody (LI-COR Biosciences, Lincoln, NE) in 1:8000 dilution. The IL-1R1 labeling was detected by the Odyssey Infrared Imaging System (LI-COR Biosciences). The strength of the signal is reported as the integrated intensity.

EAE induction and assessment

Active EAE was induced according to a previously described protocol (Stromnes and Goverman, 2006). Briefly, each mouse was anesthetized and injected subcutaneously at the base of the tail with 200 μg murine myelin oligodendrocyte glycoprotein (MOG) peptide (MOG 79–96) (Princeton Biomolecules, Langhorne, PA) in 200 μl PBS emulsified 1:1 with CFA containing 500 μg/ml inactivated *Mycobacterium tuberculosis.*

Each mouse also received 200 ng of pertussis toxin (List Biological Laboratories, Campbell, CA) i.p. at the time of immunization and 48 h later. The animals were observed for clinical signs of disease for 40–60 days. The following scale was used as a guide to score clinical manifestations of EAE: 1- tail weakness or ataxia, 2- limp tail and ataxia, 3- ataxia and starting to drag one hind leg, 4- dragging both hind legs, 5- death. The clinical score was recorded in 3 separate EAE experiments in both WT FVB and eIL-1R1 kd animals. The first two included 5 animals/group and the third included 7 animals/group.

Immunohistochemistry (IHC) and histopathology

Brains from icv IL-1-injected animals were used for IHC labeling of COX-2 expression. Lumbar spinal cords from EAE mice were used for IHC labeling of CD45, CD3 and VCAM-1. Briefly, tissue samples were snap-frozen in cold isopentane. Brain and spinal cords tissues were cryostat-cut to 20-μm-thick or 40-μm-thick sections, respectively. The sections were fixed in an acetone/alcohol mixture (3:1) for 5 min. Glucose oxidase and sodium azide were used to reduce background interference. The brain sections were then incubated with a goat anti-mouse COX-2 antibody (1:40 Cayman chemical, Ann Arbor, MI). The spinal cord sections were incubated with a rat anti-mouse CD45 (1:100, BD Pharmingen, San Diego, CA), rat anti-mouse VCAM-1 (1:10, BD Pharmingen, San Diego, CA) or rat anti-mouse CD3 (1:200, BD Pharmingen, San Diego, CA). Biotinylated rabbit anti-goat antibody (1:200 Vector Labs, Burlingame, CA) was then used to label the brain section and biotinylated rabbit anti-rat antibody (1:200 Vector Labs, Burlingame, CA) was used to label the spinal cord sections. The labeling was visualized by conventional avidin-biotin immunoperoxidase method. To quantify VCAM-1 staining from lumbar enlargement, three sections were examined from each mouse. The number of stained blood vessels in the entire section was counted. Spinal cord tissue was also stained with H&E for examination of histopathology. For H&E, CD45, CD3, and VCAM-1 labeling, animals were sacrificed at the onset of the EAE disease. Nine animals/group (FVB WT and eIL-1R1 kd) were used in this experiment.

Proliferation and IL-17 assays in unchallenged mice

Spleens were collected from both eIL-1R1 kd and FVB WT littermates. They were pressed through a 70 μm nylon strainer and washed with HBSS buffer. Cell pellets were treated with Red Blood Cell lysis buffer containing NH_4Cl to delete red blood cells. The resulting splenocytes were then washed and pressed through a 70 μm nylon strainer again. RPMI1640 culture medium with 10% FBS was used to culture the splenocytes. After they were plated into 96 wells, splenocytes ($4\times10^5/100$ μl) were stimulated with 1 ng/ml IL-1α, 100 pg/ml IL-23, or IL-23 together with IL-1α. Supernatants were collected after 4 days and IL-17 concentrations were determined by using an IL-17 ELISA kit (R&D systems). In a companion cell plate, [^{3}H] thymidine was added at the end of day 3 and the cells were harvested on day 4 to assess proliferation by [^{3}H] thymidine incorporation.

Antigen-specific leukocytes activation in immunized animals

Splenocytes were also collected ten days after animals were immunized with MOG_{79-96} peptide. They were stimulated with 10 μg/ml MOG_{79-96} peptide or culture medium *ex vivo*. Supernatants were collected 2 days later and IL-17 concentrations were determined by ELISA. In a companion culture plate, MOG stimulated proliferation was assayed by [^{3}H] incorporation described above.

Statistical Analysis

Data are presented as the means±SEM. Two-way ANOVA was performed in order to compare the entire curves of EAE clinical scores between FVB and eIL-1R1 kd animals. One-way ANOVA was used to analyze changes in the number of VCAM-1 positive blood vessels, and onset of disease. Cytokine levels and levels of proliferation were compared with un-pared student t-test. The test results were considered significant if $P<0.05$.

Results

Figure 1B shows that the two co-transgenes, Tie2-antiIL-1R1 and Tie2-GFP, can be clearly detected in the founder animal. Fig. 1Ca shows that in the brain of eIL-1R1 kd animals GFP expression was found in cells exhibiting the pattern of blood vessel cells. The GFP expressing cells are co-localized with the endothelial cell marker PECAM (Fig. 1Ca, inset). In addition, the mRNA for the antiIL-1R1 was also detected in the tail RNA of the founder animal; the level of antiIL-1R1 was about 1/16 of that expressed by the housekeeping gene G3PDH. Transgene expression can also be located in the thymus (Figure 1Cb) and spleen (Figure 1Cc). Again, the pattern of transgene expression shows an exclusive endothelial pattern in these tissues. For comparison, CD3 labeled T cells in the spleen of the transgenic animals is shown in Figure 1Cd; these labeled T cells clusters in the T cell rich region in the spleen, showing an apparent qualitatively different pattern of distribution from that of the transgene expression.

We then examined whether expression of antiIL-1R1 in brain endothelial cells inhibited the function of eIL-1R1 in eIL-1R1 kd animals. Figure 2 shows the results of COX-2 labeling in the brain after icv injection of IL-1. The data represent the patterns in the entire brain rather than that localized to a specific region. In WT FVB animals, COX-2 expression is highly associated with the blood vessels (Fig. 2A). In contrast, almost no induction of COX-2 was found in eIL-1R1 kd, which was generated from the founder FVB strain. (Fig. 2B).

To verify whether the specificity of IL-1R1 blockade in eIL-1R1 kd animals is restricted to endothelial cells, we analyzed IL-1R1 expression in leukocytes by in-cell Western. Leukocyte expression of IL-1R1 was detected in WT animals as well as eIL-1R1 kd animals (Fig. 3). No detectable change in IL-1R1 levels was found in leukocytes from eIL-1R1 kd

mice, providing evidence that the antiIL-1R1 transgene expression did not knock down IL-1R1 expressed in non-endothelial cells. Importantly, no IL-1R1 was detected in leukocytes collected from IL-1R1 KO animals (data not shown), demonstrating that the in-cell Western method specifically detected the presence of IL-1R1.

We then tested EAE disease progression in the eIL-1R1 kd mice and their WT littermates. The clinical signs of EAE were monitored daily and scored. Results from three separate experiments were combined. The averages of the scores are presented in Fig.4. In WT FVB littermates, the incidence of disease is 88% (15 of 17) and the average time of the EAE onset is 10.2 (10.15±0.6) days. In addition, the WT littermates exhibited a second relapse. In this group, the maximum clinical severity (between 1.5 and 2) was reached on day 12. The majority of WT mice recovered briefly from the initial episode, but had significant disease exacerbation during disease relapses. The WT FVB mice never completely recovered from the disease throughout the observation period. In the eIL-1R1 kd mice, the incidence is 53% (9 of 17). Eight transgenic mice never developed any clinical symptoms. The average time of onset of the other seven transgenic animals is 12.2 (12.3±0.7) days, which is significantly delayed compared with the WT FVB littermates (F (1,22) = 7.85, p=0.012). The disease severity of EAE in eIL-1R1 kd animals is decreased when compared with WT FVB littermates (two-way ANOVA, F (1,384) = 126.5, p<0.05). Unlike the FVB WT littermates, all mice in the eIL1-R1 kd group recovered completely from disease by day 36 and disease did not progress to a relapsing phase (Fig. 4).

Histopathological findings are presented in Figure 5. H&E staining shows inflammation and perivascular cuffing in the spinal cord tissue in the control FVB animals 10 days after immunization (Figure 5a), but not in eIL-1R1 kd animals (Figure 5A). Likewise, leukocyte (CD45^{+} labeled cells) infiltration in the lumbar spinal cord at the onset of EAE was found near blood vessels and meninges in FVB control animals (Fig.5b). In contrast, almost no CD45^{+} cells were observed in eIL-1R1 kd animals (Fig. 5B). No detectable CD45^{+} cells were found in the lumbar spinal cord of normal non-immunized mice (data not shown). Similarly, at the onset of EAE, CD3^{+} T cells were detected in the spinal cord in the control FVB animals (Figure 5c), but not in eIL-1R1 kd animals (Figure 5C).

We next examined the expression of VCAM-1 in the spinal cord at the onset of EAE development (day 10 after the immunization in WT animals and day 12 in eIL-1R1kd animals). In the WT FVB littermates (Fig. 5d), VCAM-1 is induced on blood vessel cells. In eIL-1R1 kd animals (Fig. 5D), VCAM-1 is also induced on blood vessel cells. However, the number of VCAM-1 positive blood vessels are significantly less in eIL-1R1 kd animals (17.9±2.3 vs 35.2±6.7; F(1,17) = 407, p<0.02).

To verify that that the loss of IL-1R1 on endothelial cell do not alter critical EAE-related responses in immune cells to IL-1, splenocytes from both FVB control and eIL-1R1 kd animals were tested for their ability to produce IL-17 and to proliferate when they are stimulated by IL-1 and IL-23. Figure 6A shows that both IL-1 and IL-23 induced increased production of IL-17 from splenocytes (t-test, p<0.05, comparing cytokine-treated cells to medium-treated cells). IL-1 and IL-23 synergistically induced highest amounts of IL-17 production. No different, however, was detected from the responses between wild type and the eIL-1R1 kd splenocytes. Figure 6B shows that IL-1 induced proliferation of splenocytes in both groups of animals. Again IL-1 and IL-23 synergistically induced the highest amounts of splenocytes proliferation. These splenocyte responses were not different between the non-transgenic FVB and the eIL-1R1 kd animals.

Next, antigen specific response to MOG was examined in splenocytes from animals challenged with MOG immunization 10 days prior. Figure 7A shows MOG stimulation of

splenocytes from previously challenged animals induced the production of IL-17. The induced IL-17 levels were not different between wild type FVB and eIL-1R1 kd splenocytes. No IL-17 induction was detected in both groups of animals if they were not sensitized with a previous MOG immunization (data not shown). Similarly, Figure 7B shows the MOG stimulation in the sensitized splenocytes induced significant proliferation. Again, no difference was detected between wild type FVB and eIL-1R1 kd splenocytes.

Discussion

We have previously generated an endothelial IL-1R1 (eIL-1R1) knockdown mouse using the Tet-on system (Ching *et al.*, 2007). In that model, eIL-1R1 was knocked down when animals received doxycycline (Dox) in their drinking water. It is well known that Dox has profound effects on the central nervous system (CNS). In particular, Dox can block microglia activation (Lai and Todd, 2006) (Cho *et al.*, 2009). Because involvement of microglial cells is evident in EAE pathogenesis as well as in a host of other CNS inflammatory states (O'Brien *et al.*, 2008), it is important to develop a model that does not require Dox and thereby eliminate the confounding effects of Dox on microglial cells. We chose to generate a transgenic mouse which produces antisense IL-1R1 constitutively in endothelial cells for this study.

The results show that GFP (as the transgene location marker) in the transgenic mice was expressed exclusively in the endothelial cells. Because co-injected transgenes typically co-integrate into the same site in the genome and both Tie2-GFP and Tie2-antiIL-1R1 were constructed to be controlled by the endothelial specific promoter-enhance, Tie2, the GFP expressing cells in the transgenic animal should also indicate the cells that express antiIL-1R1. We have bred this strain of transgenic animals for over five generations and the co-transgenes, antiIL-1R1 and GFP never separated in the offspring, indicating co-integration and co-expression of these transgenes. In a previous study, we showed that anti-IL-1R1 expression under Tie2 promoter control causes endothelial specific knockdown of IL-1R1 (Ching *et al.*, 2007). That study also showed that the most sensitive functional indication of the effectiveness of eIL-1R1 blockade in the transgenic animals is the reduction of endothelial COX-2 expression in the brain after they received icv IL-1 injection. In the current study, endothelial specific IL-1R1 knockdown is also verified by the COX-2 induction experiment: icv IL-1- induced endothelial COX-2 expression was abrogated in eIL-1R1 kd mice. On the other hand, IL-1R1 expression on blood leukocytes was preserved (Fig. 3), suggesting IL-1R1 was knocked down specifically in endothelial cells.

An important point to clarify is that the Tie-2 promoter-enhance will direct the transcription of genes during development in hematopoietic stem cells. Crossing Tie-2-Cre mouse with a Cre-reporter mouse results in offspring with the expression of the reporter gene in many leukocytes and endothelial cells (Constien *et al.*, 2001). In adult mice, however, the specific Tie2 promoter-enhance we used in the present study directs expression of transgene exclusively endothelial (Schlaeger *et al.*, 1997) (Motoike *et al.*, 2000) (Ohtsuki *et al.*, 2005) (Tam *et al.*, 2009), therefore, the eIL-1R1 kd mice we created might express antiIL-1R1 during development in cells other than endothelial cells, but they express the antiIL-1R1 exclusively in endothelial cells as adult. This is supported by the fact that the transgene marker in the adult animals showed exclusive endothelial pattern in the brain, thymus, and spleen.

Several previous studies showed that blocking the activity of IL-1 may be beneficial for EAE. Martin et al. were the first to demonstrate that inhibition of IL-1 activity by IL-1Ra effectively reduce EAE clinical signs in rats (Martin and Near, 1995). The same conclusion

was reached by Badovinac et al. who showed that IL-1Ra treatment suppresses EAE by reducing the activation and proliferation of encephalitogenic cells (Badovinac *et al.*, 1998). In addition, IL-1R1 KO mice were used in two different studies; one showed mice lacking IL-1R1 did not develop clinical signs of EAE and any evidence of lesion in the CNS (Schiffenbauer *et al.*, 2000) and the other a significant decrease in EAE incidence in IL-1R1 KO mice (Sutton *et al.*, 2006).

Two different mechanisms can be found to explain why blocking IL-1 activity may reduce EAE symptoms. In an elegant study, Sutton et al. found that EAE incidence and clinical symptoms were reduced in IL-1R1 KO animals. This was correlated with a failure to induce antigen-specific ThIL-17 cells. Further, EAE was induced in IL-1R1 KO mice by adoptive transfer of autoantigen-specific cells from wild-type mice with EAE. These results led to the conclusion that IL-1 is critical in the induction of antigen-specific ThIL-17 cells during EAE(Sutton *et al.*, 2006). Therefore, one mechanism by which blocking IL-1's activity reduces EAE symptoms is that such blockade abrogated the critical IL-1 action on peripheral T cells.

Another mechanism is based upon the activity of IL-1 within the central nervous system (CNS). Numerous studies showed that IL-1 acting in the CNS is involved in neural tissue damage following neuroinflammation (Basu *et al.*, 2004). In EAE, IL-1 is known to be induced in CNS glial cells (Bauer *et al.*, 1993) (Xiao *et al.*, 1998) and gene therapy with centrally administered IL-1Ra-expression vector ameliorated EAE symptoms (Furlan *et al.*, 2007). Therefore, IL-1 receptor within the CNS tissue, rather than on peripheral T cells, could be another critical factor during EAE induction. In this context, eIL-1R1 is especially important because in CNS tissue the most salient sites for IL-1 binding(Ban *et al.*, 1991) and IL-1R1 mRNA(Ericsson *et al.*, 1995) expression have been located to the endothelial cells. Further, we showed previously that eIL-1R1 play a critical role in mediating the recruitment of neutrophils and T cells across the BBB during neuroinflammation (Ching *et al.*, 2005) (Ching *et al.*, 2007).

The results of the present study that EAE induction is successfully inhibited in eIL-1R1 kd mice is consistent with the second mechanism that eIL-1R1 is critical in the development of EAE, probably by influencing leukocyte infiltration into the CNS tissue.

A caveat to consider here is eIL-1R1 kd mice may show reduced IL-1R1 mediated activity in cells other than endothelial cell due to the expression of Tie2-directed anti-IL-1R1 expression in hematopoietic cells during development. We therefore tested whether splenocytes from eIL-1R1 kd animals can respond to IL-1. The striking results are: 1) the splenocytes in eIL-1R1 kd mice are fully competent in producing IL-17 after IL-1, IL-23, or IL-1+IL-23 stimulation; 2) the splenocytes in eIL-1R1 kd mice show proliferation after stimulation with IL-1, and IL-1+IL-23; and 3) the splenocytes in MOG immunized eIL-1R1 kd mice produce IL-17 and proliferate after a second MOG stimulation ex vivo. No difference was detected in all these three tests between eIL-1R1 kd and the wild type FVB animals. These results strongly support the notion that IL-1-mediated IL-17 production is not the mechanism by which eIL-1R1 kd mice showed reduced EAE symptoms.

Although circulating leukocytes rarely traffic into normal CNS tissue, a high number of immune cells gain access to the CNS during EAE. This is not due to a simple breakdown of the BBB and a subsequent passive diffusion of peripheral immune cells into the CNS, because T cells found in the CNS are phenotypically distinct from T cell populations found in other inflamed organs (Engelhardt *et al.*, 1998). Instead, pertinent immune cells are actively recruited into the CNS during EAE, resulting from a cascade of leukocyte-endothelium interactions at blood-brain barrier (BBB) (Engelhardt, 2008). The vascular cell

adhesion molecule-1 (VCAM-1) plays an important role in this cascade. Vajkoczy et al. were the first to show that α4-integrin-VCAM-1 binding mediates capture of encepholitogenic T cells to the CNS microvessels (Vajkoczy *et al.*, 2001). VCAM-1 is known to be upregulated in EAE (Weller *et al.*, 1996) and pretreatment with an antibody against α4-integrin, the primary ligand of VCAM-1, can effectively block EAE development (Theien *et al.*, 2001). Endothelial IL-1R1 is critical in this cascade because IL-1 is a potent inducer of VCAM-1 expression in endothelial cells (Beekhuizen *et al.*, 1992). In the present study, the result that VCAM-1 expression in eIL-1R1 kd mice is reduced suggest that blocking IL-1-mediated VCAM-1 expression may partially account for the diminished leukocyte infiltration in these animals.

It should be noted that EAE was induced in the FVB strain in this study. FVB is an EAE resistant strain, although previous studies showed that relapsing EAE can be induced in this strain (Baker *et al.*, 2000). FVB strain was chosen because it is much easier to produce transgenic mouse in this strain. The clinical scores observed in the wild type FVB animals are lower than those found in EAE susceptible strains in the literature. However, the results were highly reproducible in three different tests and reduction in EAE symptoms in eIL-1R1 kd (on the FVB background) mice were readily observable each time.

The findings reported here show that knockdown of eIL-1R1 results in a decrease in incidence, severity and a delayed onset of EAE. In addition, mice lacking functional eIL-1R1 show a significant decrease in VCAM-1 expression and reduced CD45^{+} leukocytes in the CNS of animals with EAE. Taken together, these findings indicate a critical role for eIL-1R1 mediated pathogenesis in EAE, and describe a new model that can be used to study eIL-1R1.

This study adds a cell type specific dimension to the role of IL-1 in EAE. Although anti-IL-1 treatment as a therapy for MS has received overwhelming support in the literature from animal model studies, currently, no report has shown that anti-IL-1 treatment is effective in treating human MS (Warabi, 2007). The result of this study suggest that instead of blocking all of IL-1-mediated effects, focusing specifically on IL-1-mediated effects on endothelial cells could be an alternative strategy for the treatment of MS.

Research Highlights

In this study, we created a transgenic mouse (eIL-1R1 kd) in which IL-1R1 expression is knocked down specifically in endothelial cells. Induction of EAE in eIL-1R1 kd mice results in a decrease in incidence, severity and delayed onset of EAE. In addition, eIL-1R1 kd mice show significant decrease in VCAM-1 expression and diminished CD45^{+} and CD3^{+} infiltrating leukocytes in the spinal cord in animals challenged with EAE. Further, IL-1 and IL-23 stimulate IL-17 production by splenocytes from both wild type and the eIL-1R1 kd animals. Similarly, IL-1 and IL-23 synergistically stimulate splenocytes proliferation in these two strains of animals. After immunization with MOG_{79-96}, although eIL-1R1 kd mice displayed greatly reduced clinical scores, their splenocytes produced IL-17 and proliferated in response to a second MOG challenge, similar to wild type animals. These findings indicate a critical role for endothelial IL-1R1 in mediating the pathogenesis of EAE, and describe a new model that can be used to study endothelial IL-1R1.

References

Ahmed ST, Mayer A, Ji JD, Ivashkiv LB. Inhibition of IL-6 signaling by a p38-dependent pathway occurs in the absence of new protein synthesis. J Leukoc Biol 2002;72(1):154–162. [PubMed: 12101275]

Badovinac V, Mostarica-Stojkovic M, Dinarello CA, Stosic-Grujicic S. Interleukin-1 receptor antagonist suppresses experimental autoimmune encephalomyelitis (EAE) in rats by influencing the activation and proliferation of encephalitogenic cells. J Neuroimmunol 1998;85(1):87–95. [PubMed: 9627001]

Baker AM, Grekova MC, Richert JR. EAE susceptibility in FVB mice. J Neurosci Res 2000;61(2): 140–145. [PubMed: 10878586]

Ban E, Milon G, Prudhomme N, Fillion G, Haour F. Receptors for interleukin-1 (alpha and beta) in mouse brain: mapping and neuronal localization in hippocampus. Neuroscience 1991;43(1):21–30. [PubMed: 1833666]

Basu A, Krady JK, Levison SW. Interleukin-1: a master regulator of neuroinflammation. J Neurosci Res 2004;78(2):151–156. [PubMed: 15378607]

Bauer J, Berkenbosch F, Van Dam AM, Dijkstra CD. Demonstration of interleukin-1 beta in Lewis rat brain during experimental allergic encephalomyelitis by immunocytochemistry at the light and ultrastructural level. J Neuroimmunol 1993;48(1):13–21. [PubMed: 8227304]

Beekhuizen H, Verdegaal EM, Blokland I, van Furth R. Contribution of ICAM-1 and VCAM-1 to the morphological changes in monocytes bound to human venous endothelial cells stimulated with recombinant interleukin-4 (rIL-4) or rIL-1 alpha. Immunology 1992;77(3):469–472. [PubMed: 1282495]

Brosnan CF, Cannella B, Battistini L, Raine CS. Cytokine localization in multiple sclerosis lesions: correlation with adhesion molecule expression and reactive nitrogen species. Neurology 1995;45(6 Suppl 6):S16–21. [PubMed: 7540265]

Cannella B, Raine CS. The adhesion molecule and cytokine profile of multiple sclerosis lesions. Ann Neurol 1995;37(4):424–435. [PubMed: 7536402]

Ching S, He L, Lai W, Quan N. IL-1 type I receptor plays a key role in mediating the recruitment of leukocytes into the central nervous system. Brain Behav Immun 2005;19(2):127–137. [PubMed: 15664785]

Ching S, Zhang H, Belevych N, He L, Lai W, Pu XA, Jaeger LB, Chen Q, Quan N. Endothelial-specific knockdown of interleukin-1 (IL-1) type 1 receptor differentially alters CNS responses to IL-1 depending on its route of administration. J Neurosci 2007;27(39):10476–10486. [PubMed: 17898219]

Cho Y, Son HJ, Kim EM, Choi JH, Kim ST, Ji IJ, Choi DH, Joh TH, Kim YS, Hwang O. Doxycycline is neuroprotective against nigral dopaminergic degeneration by a dual mechanism involving MMP-3. Neurotox Res 2009;16(4):361–371. [PubMed: 19582534]

Constien R, Forde A, Liliensiek B, Grone HJ, Nawroth P, Hammerling G, Arnold B. Characterization of a novel EGFP reporter mouse to monitor Cre recombination as demonstrated by a Tie2 Cre mouse line. Genesis 2001;30(1):36–44. [PubMed: 11353516]

Dinarello CA. Immunological and inflammatory functions of the interleukin-1 family. Annu Rev Immunol 2009;27:519–550. [PubMed: 19302047]

Dincic E, Zivkovic M, Stankovic A, Obradovic D, Alavantic D, Kostic V, Raicevic R. Association of polymorphisms in CTLA-4, IL-1ra and IL-1beta genes with multiple sclerosis in Serbian population. J Neuroimmunol 2006;177(1–2):146–150. [PubMed: 16769128]

Engelhardt B. The blood-central nervous system barriers actively control immune cell entry into the central nervous system. Curr Pharm Des 2008;14(16):1555–1565. [PubMed: 18673197]

Engelhardt B, Martin-Simonet MT, Rott LS, Butcher EC, Michie SA. Adhesion molecule phenotype of T lymphocytes in inflamed CNS. J Neuroimmunol 1998;84(1):92–104. [PubMed: 9600713]

Ericsson A, Liu C, Hart RP, Sawchenko PE. Type 1 interleukin-1 receptor in the rat brain: distribution, regulation, and relationship to sites of IL-1-induced cellular activation. J Comp Neurol 1995;361(4):681–698. [PubMed: 8576422]

Furlan R, Bergami A, Brambilla E, Butti E, De Simoni MG, Campagnoli M, Marconi P, Comi G, Martino G. HSV-1-mediated IL-1 receptor antagonist gene therapy ameliorates MOG(35–55)-induced experimental autoimmune encephalomyelitis in C57BL/6 mice. Gene Ther 2007;14(1): 93–98. [PubMed: 16929354]

Hauser SL, Doolittle TH, Lincoln R, Brown RH, Dinarello CA. Cytokine accumulations in CSF of multiple sclerosis patients: frequent detection of interleukin-1 and tumor necrosis factor but not interleukin-6. Neurology 1990;40(11):1735–1739. [PubMed: 2234430]

Hubbard AK, Rothlein R. Intercellular adhesion molecule-1 (ICAM-1) expression and cell signaling cascades. Free Radic Biol Med 2000;28(9):1379–1386. [PubMed: 10924857]

Lai AY, Todd KG. Hypoxia-activated microglial mediators of neuronal survival are differentially regulated by tetracyclines. Glia 2006;53(8):809–816. [PubMed: 16541436]

Martin D, Near SL. Protective effect of the interleukin-1 receptor antagonist (IL-1ra) on experimental allergic encephalomyelitis in rats. J Neuroimmunol 1995;61(2):241–245. [PubMed: 7593560]

Motoike T, Loughna S, Perens E, Roman BL, Liao W, Chau TC, Richardson CD, Kawate T, Kuno J, Weinstein BM, Stainier DY, Sato TN. Universal GFP reporter for the study of vascular development. Genesis 2000;28(2):75–81. [PubMed: 11064424]

O'Brien K, Fitzgerald DC, Naiken K, Alugupalli KR, Rostami AM, Gran B. Role of the innate immune system in autoimmune inflammatory demyelination. Curr Med Chem 2008;15(11):1105–1115. [PubMed: 18473806]

Ohtsuki S, Kamiya N, Hori S, Terasaki T. Vascular endothelium-selective gene induction by Tie2 promoter/enhancer in the brain and retina of a transgenic rat. Pharm Res 2005;22(6):852–857. [PubMed: 15948028]

Proescholdt MG, Chakravarty S, Foster JA, Foti SB, Briley EM, Herkenham M. Intracerebroventricular but not intravenous interleukin-1beta induces widespread vascular-mediated leukocyte infiltration and immune signal mRNA expression followed by brain-wide glial activation. Neuroscience 2002;112(3):731–749. [PubMed: 12074914]

Schiffenbauer J, Streit WJ, Butfiloski E, LaBow M, Edwards C 3rd, Moldawer LL. The induction of EAE is only partially dependent on TNF receptor signaling but requires the IL-1 type I receptor. Clin Immunol 2000;95(2):117–123. [PubMed: 10779405]

Schlaeger TM, Bartunkova S, Lawitts JA, Teichmann G, Risau W, Deutsch U, Sato TN. Uniform vascular-endothelial-cell-specific gene expression in both embryonic and adult transgenic mice. Proc Natl Acad Sci U S A 1997;94(7):3058–3063. [PubMed: 9096345]

Stromnes IM, Goverman JM. Active induction of experimental allergic encephalomyelitis. Nat Protoc 2006;1(4):1810–1819. [PubMed: 17487163]

Sutton C, Brereton C, Keogh B, Mills KH, Lavelle EC. A crucial role for interleukin (IL)-1 in the induction of IL-17-producing T cells that mediate autoimmune encephalomyelitis. J Exp Med 2006;203(7):1685–1691. [PubMed: 16818675]

Tam J, Duda DG, Perentes JY, Quadri RS, Fukumura D, Jain RK. Blockade of VEGFR2 and not VEGFR1 can limit diet-induced fat tissue expansion: role of local versus bone marrow-derived endothelial cells. PLoS ONE 2009;4(3):e4974. [PubMed: 19333381]

Theien BE, Vanderlugt CL, Eagar TN, Nickerson-Nutter C, Nazareno R, Kuchroo VK, Miller SD. Discordant effects of anti-VLA-4 treatment before and after onset of relapsing experimental autoimmune encephalomyelitis. J Clin Invest 2001;107(8):995–1006. [PubMed: 11306603]

Tsukada N, Miyagi K, Matsuda M, Yanagisawa N, Yone K. Tumor necrosis factor and interleukin-1 in the CSF and sera of patients with multiple sclerosis. J Neurol Sci 1991;104(2):230–234. [PubMed: 1940977]

Vajkoczy P, Laschinger M, Engelhardt B. Alpha4-integrin-VCAM-1 binding mediates G protein-independent capture of encephalitogenic T cell blasts to CNS white matter microvessels. J Clin Invest 2001;108(4):557–565. [PubMed: 11518729]

Warabi Y. Role of IL-1 and potential therapies in multiple sclerosis. Drug discovery today 2007;4(1): 19–24.

Weller RO, Engelhardt B, Phillips MJ. Lymphocyte targeting of the central nervous system: a review of afferent and efferent CNS-immune pathways. Brain Pathol 1996;6(3):275–288. [PubMed: 8864284]

Xiao BG, Bail XF, Zhang GX, Hedlund G, Link H. Linomide-mediated protection of oligodendrocytes is associated with inhibition of nitric oxide production and IL-1beta expression in Lewis rat glial cells. Neurosci Lett 1998;249(1):17–20. [PubMed: 9672378]
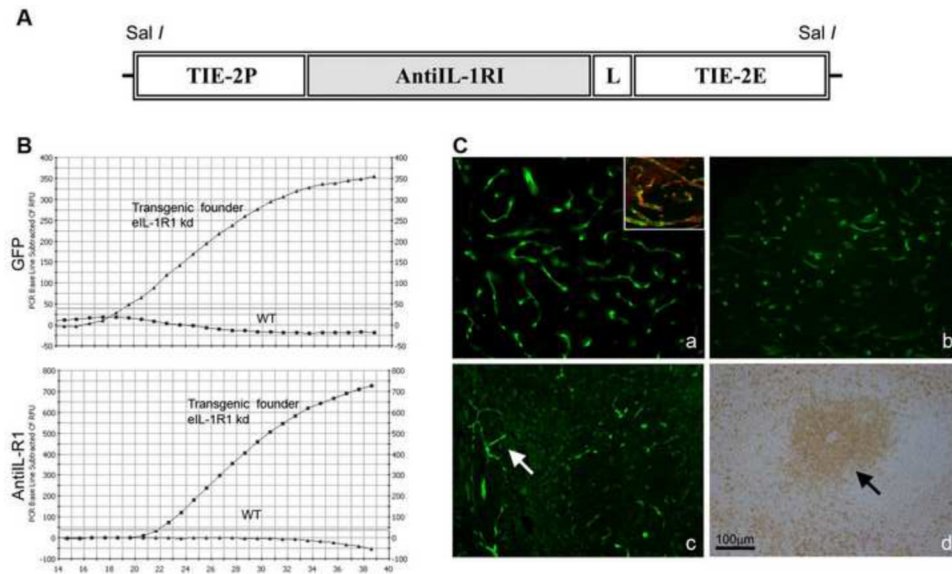
Figure 1.
A. Schematic drawing of the transgene construct for AntiIL-1R1. The antisense cDNA for IL-1R1 (AntiIL-1R1) was placed between the Tie2 promoter (Tie2P) and the Tie2 enhancer (Tie2E). L: linker sequence. B. Top, realtime PCR results show founder animal contains GFP sequence; bottom, detection of AntiIL-1R1 (via the detection of the linker sequence). These transgenes are absent in WT control animals. C. Transgene expression is found in brain (Fig. 1Ca), thymus (Fig.1Cb), and spleen (Fig. 1Cc) in endothelial cells, as indicated by the cell type-specific appearance of GFP in these cells. Fig. 1Cd show spleen CD3 labeling; CD3^{+} T cells do not show the same morphology as the transgene-expressing cells. Inset in Fig. 1Ca shows double-labeling of GFP (green) and PECAM (red) in eIL-1R1 kd brain tissue; all GFP expressing cells are co-localized with the endothelial marker PECAM.
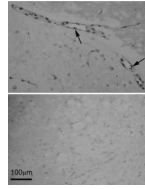
Figure 2.
Representative microphotographs show COX-2 induction in the brain 4 h after icv IL-1β injection in WT (A) and eIL-1R1 kd (B) and animals. Arrow points to labeled COX-2 positive cells.
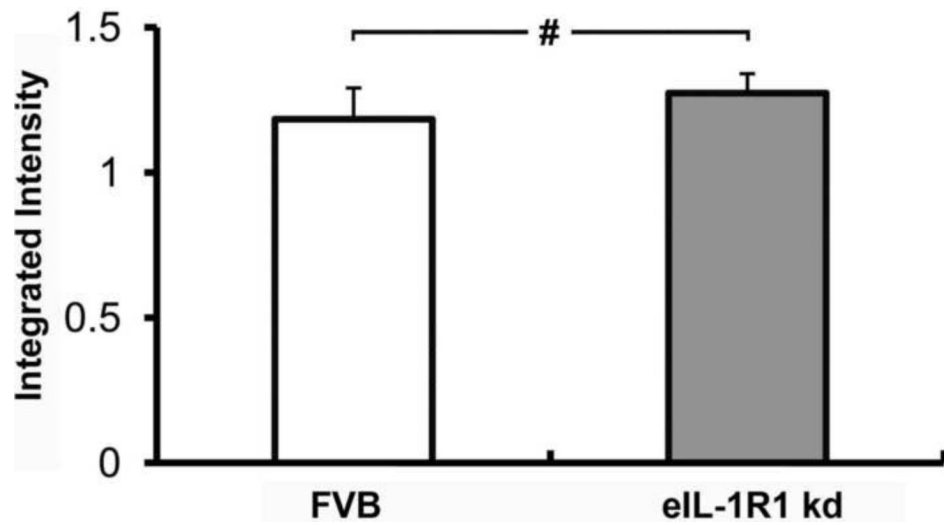
Figure 3.
Detection of IL-1R1 protein by in-cell Western in leukocytes from WT and eIL-1R1 kd
animals. # indicates no statistical difference between WT and eIL-1R1 kd leukocytes,
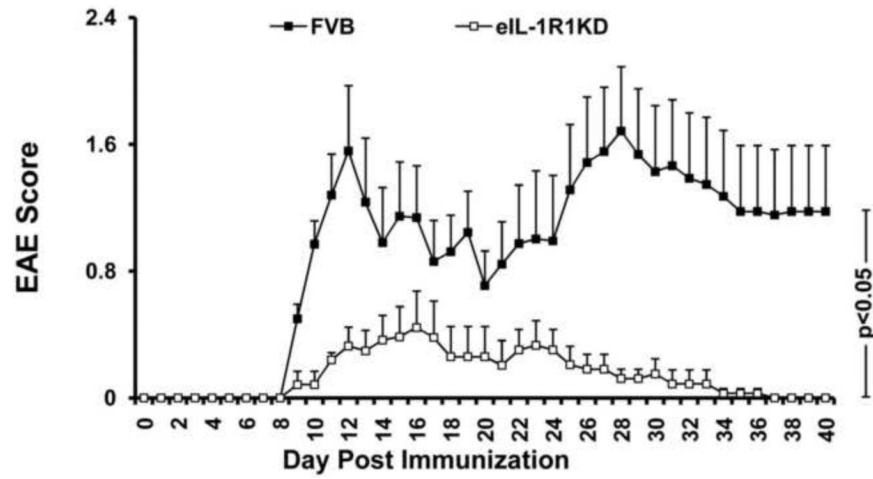p<0.05 by student t-test.

Figure 4.
Mean clinical scores of EAE symptoms in WT FVB and eIL-1R1 kd animals. Means and standard error of the mean are presented. Higher EAE scores were found in the WT FVB mice (n =17 for both groups, p<0.05 by two-way ANOVA).
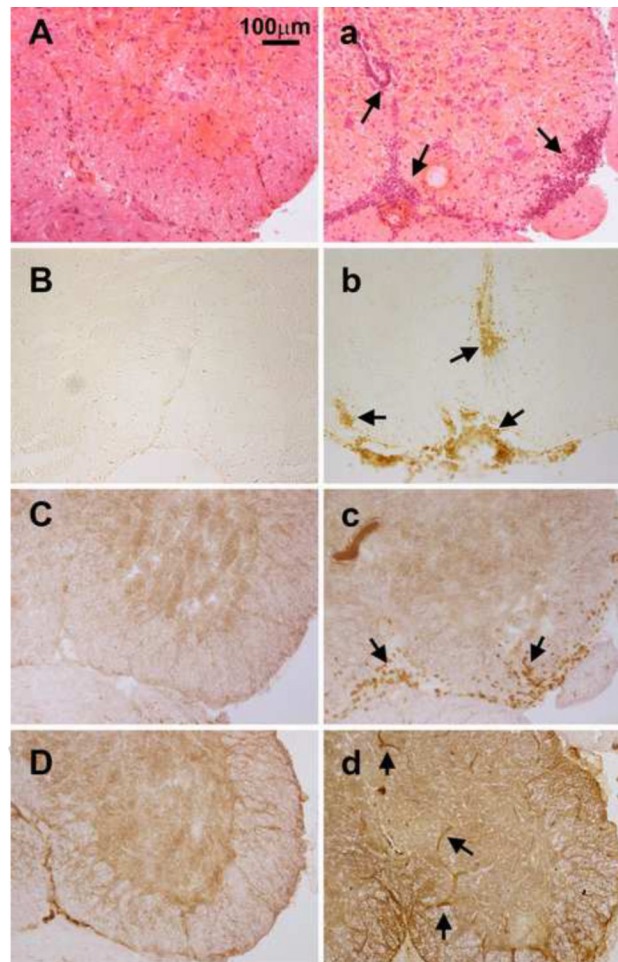
Figure 5.
Representative microphotographs of H&E stained and immunohistochemically labeled spinal cord sections at the onset of EAE. A–D are from eIL-1R1 kd animals, and a–d WT FVB animals. A and a: H&E; B and b: CD45, C and c: CD3; D and d: VCAM-1. Arrows point to areas of perivascular cuffing and spinal inflammation in Fig. 5a, CD45+ infiltrating leukocytes in Fig. 5b, CD3+ infiltrating T cells in Fig. 5c, and VCAM positive blood vessels in Figs. 5d and 5D.
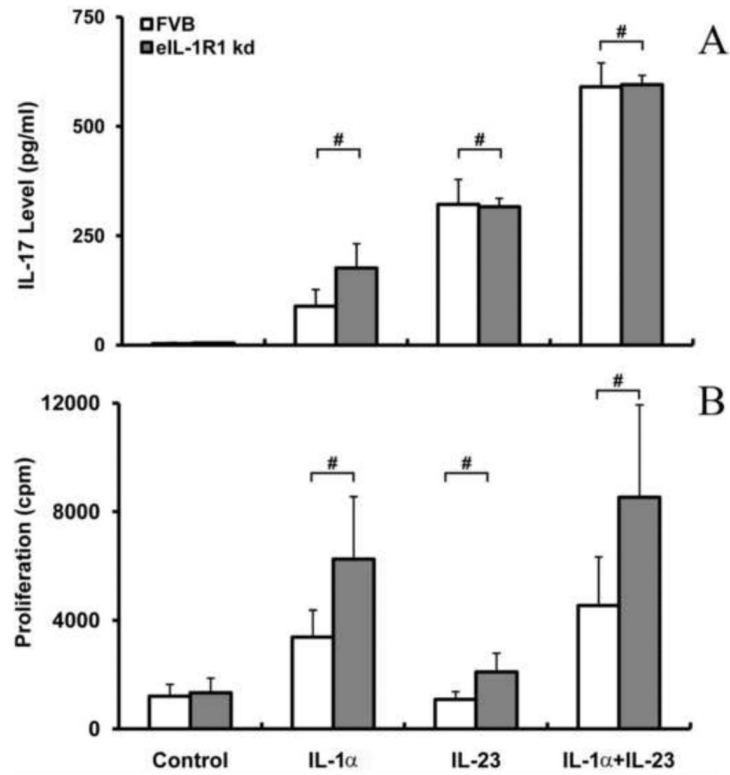
Figure 6.
IL-1 and IL-23 stimulated splenocytes responses. A. IL-17 levels after splenocytes were stimulated with IL-1, IL-23, and IL-1+IL-23. B. Proliferation of splenocytes after they were treated with IL-1, IL-23, and IL-1+IL-23. # indicates no statistical difference between results obtains from WT FVB and eIL-1R1 kd splenocytes (student t-test, p>0.05).
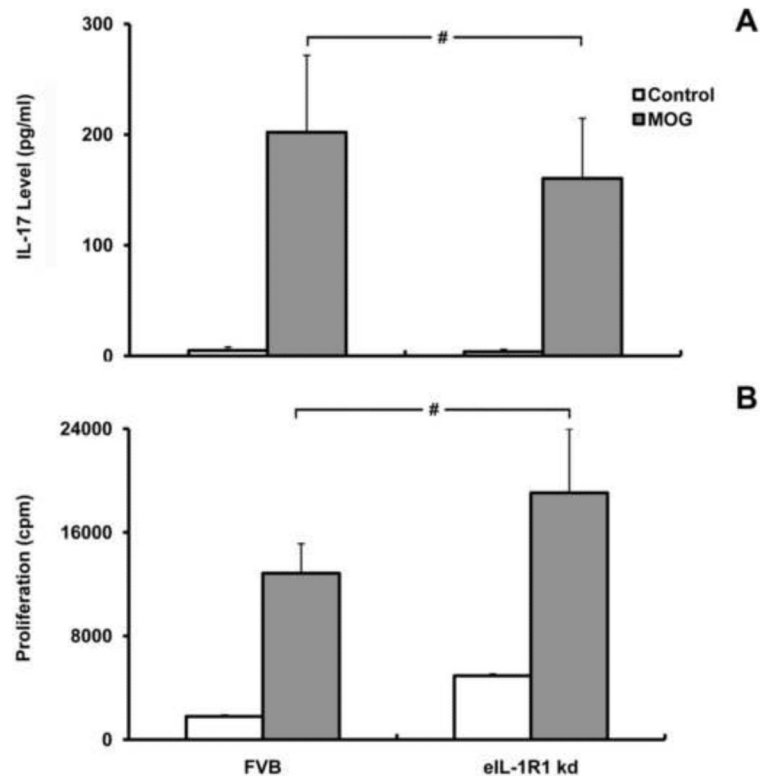
Figure 7.
Antigen specific response. A. IL-17 levels produced in response to MOG stimulation by splenocytes from animals that were previously immunized with MOG. B. Proliferation of the same sensitized splenocytes after the second MOG challenge. # indicates no statistical difference between results obtains from WT FVB and eIL-1R1 kd splenocytes (student t-test, p>0.05).